Optik - International Journal for Light and Electron Optics 271 (2022) 170022

Contents lists available at ScienceDirect

Optik

journal homepage: www.elsevier.com/locate/ijleo

The effect of V_2O_5/MgO substitution on SiO_2-Na_2O-CaO-ZnO–MgO glass structure

S. Cetinkaya Colak *

Eskisehir Osmangazi University, Faculty of Science and Letters, Department of Physics, Eskisehir, TR 26040, Turkey

ARTICLE INFO

Keywords:
Oxide glasses
V_2O_5 doped glasses
Band gap
Urbach energy
DTA analysis

ABSTRACT

V_2O_5 incorporated sodium calcium silicate glasses of composition 55SiO_2 - 25 Na_2O - 5CaO - 10ZnO - 5MgO(1-x): V_2O_5(x) (x = 0, 0.01, 0.03, 0.05, and 0.1) have been prepared by melt-quench technique. In the determination of the glass network, a silicate glass structure was chosen for physical and chemical strength. It was preferred to use ZnO for high light transmittance and V_2O_5 to reduce the optical band gap. The structural and thermal properties of the samples were explored using Fourier transform infrared (FTIR) spectroscopy and differential thermal analysis (DTA), respectively. The optical properties of the glasses were detected by UV–VIS spectroscopy between the wavelength ranges of 200–1100 nm. The indirect band gap (E_g) and Urbach energy (E_o) values have been evaluated with the help of absorption spectra. Also, the refractive index values have been determined by spectroscopic ellipsometry. All data have been interpreted corresponding with V_2O_5 contributions.

1. Introduction

Glass is a material that is widely used in several technological fields today. One of these fields is energy. Glass materials are the most preferred substrate material, especially for semiconductor materials used in photovoltaic solar cells. Changes are being made in the structures of these materials to improve the physical characteristics of the semiconductor materials used in these photovoltaic solar cells. However, the type of substrate used to produce these materials also has a significant effect on the physical properties of the material [1]. Using commercially available microscope glass, silicon, and ITO (indium tin oxide) to make these semiconductor materials limit the researcher's ability to investigate the effects of the substrate on the semiconductor film properties. Most inorganic glasses are composed of oxide-silica glasses. Silicate glasses are one of the most scientifically studied glass structures with their high light transmittance, chemical resistance, low thermal expansion, and low cost. By adding alkali, alkaline earth, and other metal oxides to SiO_2, a wide variety of two or more component glass systems can be achieved [2]. Silicate glasses with a high ZnO concentration are useful in a variety of applications, particularly in the optical sector [3,4]. A glass containing ZnO is the most ideal for a glass manufacturer because it has superior physical and mechanical qualities, including a lower softening point than other types of glasses [5]. The electrons in the outer d shells of TM ions are well known to interact significantly with the surrounding chemical environment [6–8]. TM ions exhibit wide bands in their optical spectra when compared to rare-earth ions [9,10]. V_2O_5 is one of the most intriguing and preferred TMOs for semiconducting glass production. The vanadium element's valence states V^{5+}, V^{4+}, V^{3+}, and V^{2+} are determined by the outer D-electrons. The glasses with low levels of the ratio V^{4+}/V^{5+} are classified as n-type semiconductors. Besides filling

* Corresponding author.
E-mail address: sccolak@ogu.edu.tr.

https://doi.org/10.1016/j.ijleo.2022.170022
Received 20 August 2022; Accepted 20 September 2022
Available online 22 September 2022
0030-4026/© 2022 Elsevier GmbH. All rights reserved.

gaps in the matrix and improving its characteristics, V_2O_5 may have a role in the development of the glass network [11,12]. Vanadium pentoxide is found in glasses as a glassmaker with semiconducting characteristics, making it a viable alternative for a wide range of applications [13,14].

Our aim in this study is to produce glass substrates instead of purchasing glass substrates, which have significant advantages in semiconductor structures. For this purpose, the glass structure SiO_2-Na_2O-Ca-ZnO-MgO: V_2O_5 was chosen. The effects of the substrate structure on the film will be investigated further by coating the film on the glasses examined in this article.

2. Experimental

Glasses in the structure of 55 SiO_2 – 25 Na_2O – 5 CaO − 10 ZnO – (5 – x) MgO: xV_2O_5 (x = 0, 0.1, 0.3, 0.5, 1) (all in weight %) are produced using the classical melt-quenching technique. Each glass series and its codes are given in Table 1. Appropriate amounts of chemically pure SiO_2 (Alfa Aesar, 99.8%), Na_2O (Merc, 99.9%), CaO (Alfa Aesar, 99.5%), V_2O_5 (Sigma-Aldrich, 99.8%), ZnO (Sigma-Aldrich, 99.9%) were weighed and mixed with precision. The mixture was placed in a high-temperature furnace at 1400 °C in a pure platinum crucible. The glasses, which were kept in the high-temperature furnace for 5 h by shaking with an interval of half an hour, were shaped by pouring into a cylindrical graphite mold at the end of melting and immediately transferred to the annealing oven at 450 °C. It was kept in the annealing furnace at 450 °C for 1 h and then the oven was left to cool down to room temperature. The resulting glasses were meticulously cut and polished for optical measurements (Fig. 1), and powdered for IR and DTA evaluations.

Densities of produced glass samples were determined by the Archimedes method at room temperature, using an analytical balance with 0.0001 g precision, OHAUS AX224 brand analytical balance, density kit, and ethanol ($\rho_e = 0.784 gcm^{-3}$ at 26 °C). Transmittance and absorbance spectra were measured between the range of 200–1100 nm in 2 nm steps at room temperature with a UNICO UV–Vis spectrophotometer. FTIR spectra were obtained with Perkin Elmer Spectrum Two device between the range of 400–1600 cm^{-1} at room temperature with a resolution of 4 cm^{-1} and diamond ATR was used in this analysis. Differential thermal analysis (DTA) measurements were performed using a Perkin Elmer TG/DTA 6300 analyzer at a temperature range of 30–1300 °C, at a rate of 10 °Cmin^{-1} under a dynamic nitrogen gas atmosphere.

3. Results and discussion

3.1. Density and molar volume measurements

Density and molar volume values are important data in explaining the physical properties of glasses. Accurately and quickly measurable (up to three steps, even in a medium-equipped laboratory) and is often used in quality control of commercial glass production [15]. The density depends on the modification of the geometric configurations of the glass mesh, the variation in coordination, and the size of the interstitial spaces [16]. The densities of the glass samples were calculated using the following formula:

$$\rho = \frac{W_a}{W_a - W_e} \cdot \rho_e \quad (1)$$

where W_a is the sample weight measured in the air; W_e is the sample weight measured in ethanol, and ρ_e is the density of the immersion liquid in which the experiment is performed.

The molar volumes (V_m) of the produced glasses were calculated using the following formula:

$$V_m = \frac{\sum X_i M_i}{\rho} \quad (2)$$

where x_i is the molar fraction and M_i is the molecular weight of the i_{th} component.

Measured density and calculated molar volume values are given in Table 1. In general, the main factors affecting the density of the glass are the size and weight of the contributed material. [16]. When Table 1 is examined, when V_2O_5 is doped to the base glass structure, it is seen that the density values decrease slightly as a result of the substitution of MgO and V_2O_5. Since the density of V_2O_5 is 3.36 g/cm^3 and the density of MgO is 3.58 g/cm^3, it is natural to observe a decrease in density values. In general, density and molar volume are expected to show opposite behavior. This relationship is seen in the glasses we prepared and the molar volume values have increased. Thus, we conclude that as the amount of V_2O_5 doping increases, there is an increase in bond lengths or interatomic spacing between glass atoms.

Table 1
Compositions (wt%), Density (ρ), and molar volume (V_m) values of the produced glasses.

Sample Code	Composition Detail (wt%)	d (g.cm^{-3})	V_m ($cm^3.mol^{-1}$)
S-0	55SiO_2 - 25Na_2O - 5CaO − 10ZnO - 5MgO	2.73	22.49
S-01	55SiO_2 - 25Na_2O - 5CaO - 10ZnO - 4.9 MgO - 0.1 V_2O_5	2.72	22.68
S-03	55SiO_2 - 25Na_2O - 5CaO - 10ZnO - 4.7MgO - 0.3 V_2O_5	2.72	22.86
S-05	55SiO_2 - 25Na_2O - 5CaO - 10ZnO - 4.5MgO - 0.5 V_2O_5	2.70	22.94
S-1	55SiO_2 - 25Na_2O - 5CaO - 10ZnO - 4 MgO - 1 V_2O_5	2.69	23.02

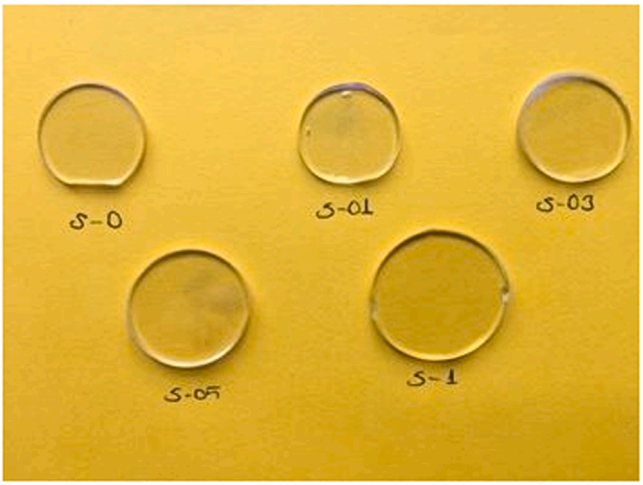


Fig. 1. The photographs of the produced glasses.

3.2. FT-IR measurement

Especially in glass and ceramic materials, the FT-IR absorption spectrum plays an important role, as it is a powerful tool that carries information including molecular vibration or rotation to determine the nature of chemical bonds and related coordination groups. [17]. Fig. 2. shows the FT-IR spectrum of the produced glasses, recorded between 250 cm^{-1} and 3000 cm^{-1}.

Some minor changes in the spectrum were observed with increasing vanadium oxide content in the FTIR spectrum. We can say that the spectrum consists of two parts. The first is the 400–1200 cm^{-1} (middle IR) region formed by large and prominent peaks, and the other is in the region between 1200 and 3000 cm^{-1} where small peaks observed with V_2O_5 doping are observed. In the literature, studies on silicate glasses indicate that there are high-intensity vibration modes between 800 and 1200 cm^{-1}, low-intensity vibration modes between 600 and 800 cm^{-1} and medium-intensity vibration modes between 400 and 600 cm^{-1} [18–23]. The FTIR spectrum of the glasses we produce is in harmony with the literature. The area ranging from 400 to 600 cm^{-1} is related to the bending modes of the

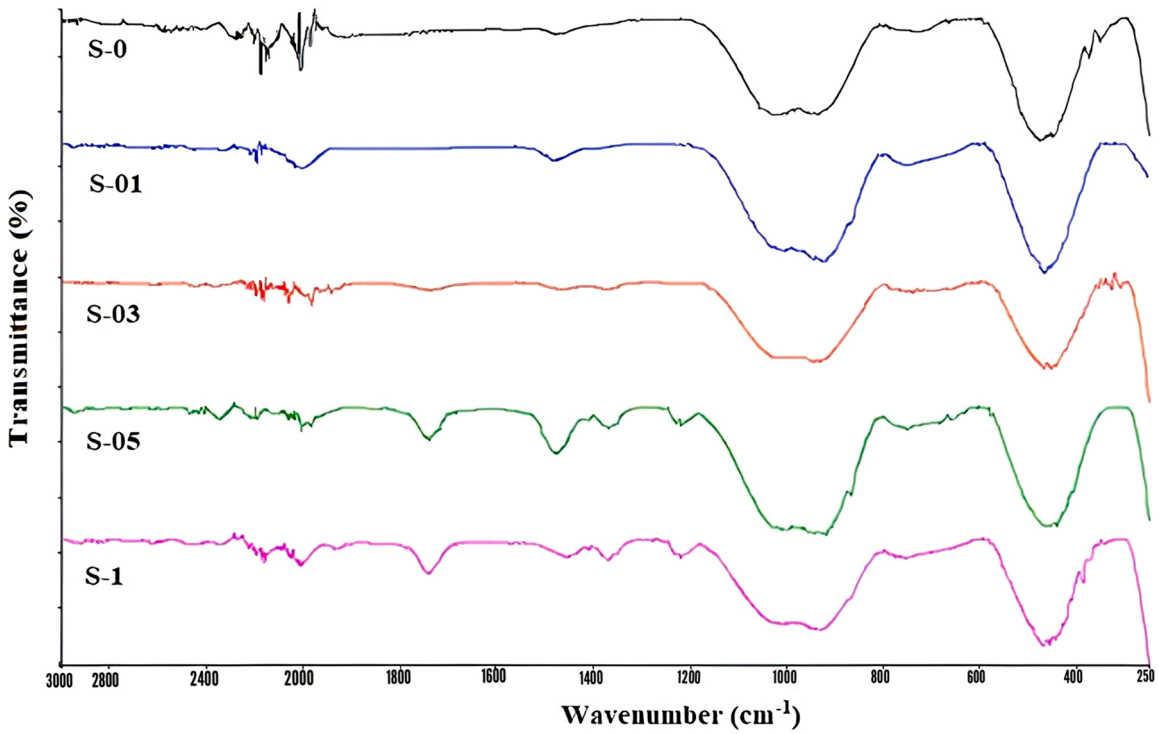


Fig. 2. FT-IR spectrum of produced glasses.

bridging oxygen (BO) in the glass network of Si−O−Si and O−Si−O. Also in this region, transmittance bands in the range of 400–460 cm^{-1} correspond to the Zn-O stretching vibration bond. The second sub-region, varying between 600 and 800 cm^{-1}, is associated with reduced Si−O stretch bonds due to the lower concentration of the SiO tetrahedron [24]. From the spectrum, it is seen that the vibration modes in this region decrease with the increase of V_2O_5 in the glass structure. Also, as the amount of V_2O_5 increased, the transmittance band in this region widened and shifted towards a higher wavenumber. This means the bending vibration of the Zn−O−Si bond and the Si−O−Si structure deformation [25,26]. The last sub-region extending from about 800–1200 cm-1 is the stretching vibrations of the SiO_4 and ZnO_4 tetrahedron [27,28]. Unlike the literature, one more distinctive peak draws attention to the produced glasses in this region. These peaks ranging from 913 cm^{-1} to 945 cm^{-1} are assigned to antisymmetric stretching or stretching vibrations of Si-O and are probably related to the presence of diopside ($MgCaSi_2O_6$) [16]. This peak intensity increased until 1% V_2O_5 doping, but the peak intensity decreased in 1% V_2O_5 doped S-1 glass. And while these peak values shift to low wavenumber until S-1 glass, in S-1 glass; took the value of wavenumber in the base glass structure. As a result, as the amount of V_2O_5 doping to the base glass composition increased, up to 1% doping, the amount of non-bridging oxygen (NBO) increased due to the formation of V-O-V bonds. In 1% V_2O_5 doped S1 glass, the doped vanadium oxide acted as a glass-former and the amount of NBO in the structure decreased. It is thought that the small-intensity peaks, which are visible in S-05 and S-1 glasses at wavenumbers higher than 1200 cm^{-1}, belong to the OH groups in the glass structure.

3.3. Optical properties

3.3.1. Transmittance spectrum

The transmittance spectra of undoped and V_2O_5 doped silicate glass structures are given in Fig. 3. When the graph is examined, with the gradual addition of V_2O_5, the absorption edge showed a redshift. Presumably, the redshifts are due to the accumulation of negative acting charge on oxygen with increasing size of vanadium oxide clusters [29]. The transmittance of the glasses in the visible region is around 90% and the V_2O_5 doping did not reduce the transmittance. This is a desirable feature to have as a substrate for the production of materials that can be used in solar cell applications.

3.3.2. Examination of electronic band structures

The optical band gap of the prepared glasses was procured from the Davis and Mott equation derived from the absorption edge using the equation:

$$\alpha h\upsilon = B(h\upsilon - E_g)^{n}$$

α is the absorption coefficient, B is an energy-independent constant, hν is the photon energy, E_g is the optical band gap in eV and n is an index representing the mechanism of interband transitions, i.e., n = 2 and n = ½ for indirect allowed transitions and direct allowed transitions, respectively. Using the above equation and plotting $(\alpha h\nu)^{1/2}$ and $(\alpha h\nu)^2$ as a function of photon energy hν, the optical band gap (E_g) values can be found for the indirect and direct transitions, respectively. The corresponding value of E_g is obtained by achieving the linear part of the graph $(\alpha h\nu)^{1/2} = 0$ for indirect transitions and $(\alpha h\nu)^2 = 0$ for direct transitions. Since the transitions are known to be indirect for amorphous structures in general and glasses in particular, optical band gaps for indirect transitions (n = 2) were calculated in this article. Fig. 4 gives the graphs $(\alpha h\nu)^{1/2} \sim h\nu$ used to calculate the optical band gap of the silicate-based glass structures produced. In addition, optical band gap values calculated using these graphs are given in Table 2. Optical band gap values of the produced glasses vary between 3.668 eV and 3.315 eV. As the V_2O_5 doping increases, it is seen that there is a remarkable decrease in the optical band gap (E_g) value of the glass structures up to the S-1 glass. This means that the glass mesh structure changes due to the intervention of V_2O_5 as a contributor to the glasses. Moreover, the indirect transition is approximately present where the vanadium ions act as defect centers near the Fermi level and the direction of the transition will be from the valence band to the vanadium zones

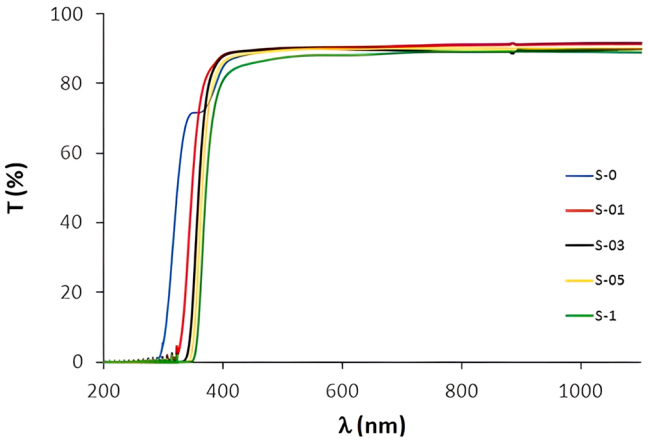


Fig. 3. The transmittance spectrum of the produced glasses.

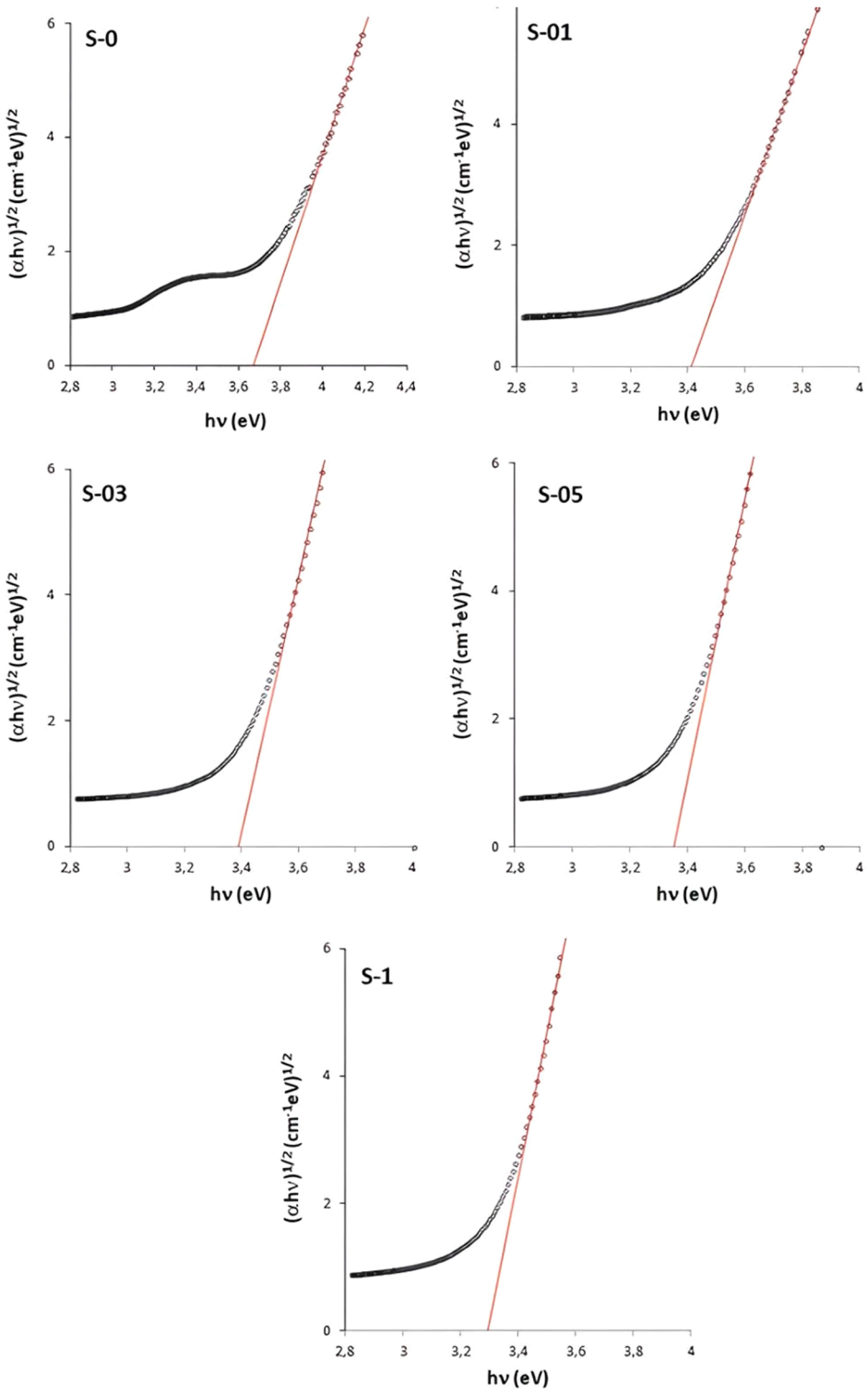


Fig. 4. $(\alpha h\nu)^{1/2} \sim h\nu$ graphs of the produced glasses.

and finally from the defect region to the conduction band. Previous work on glasses containing transition metal ions confirms the current work on the generation of non-bridging oxygens, this means that a modified structure is obtained with such glasses [30–33]. It is thought that this situation is due to the increase in non-bridging oxygen density as a result of the V_2O_5 entering the network structure and acting as a network modifier. No significant change was observed in the E_g value of 1% V_2O_5 doped S-1 glass. With this result, it is

Table 2
The indirect band gap (E_g), Urbach energy (E_o), refractive index, and average extinction coefficient values of the produced glasses.

Sample Code	E_g (eV)	E_o (eV)	$n_{(600\ nm)}$	k_{ort}
S-0	3668	0206	1.912	0.005
S-01	3415	0144	2.227	0.003
S-03	3391	0114	2.234	0.004
S-05	3348	0104	2.264	0.007
S-1	3315	0098	1.916	0.006

thought that the 1% V_2O_5 contribution that enters the structure plays a network-forming role.

In the area just below the area where strong absorption occurs, when the absorption coefficient is analyzed for energy change, an idea of the width of localized levels can be obtained. For this purpose, the values of Urbach energy (E_o) were calculated by drawing the $\ln \alpha \sim h\nu$ graphs given in Fig. 5 for silicate-based glass structures (Table 2). As shown in the table, samples containing V_2O_5 show a reduction in the contribution amount of E_o values showing the width of localized levels. The low values of Urbach energy tell us that the glass is steady and stable. The increase in the V_2O_5 ratio in the glass network makes the structure neat and stable.

3.3.3. Determining the optical constants of the glass structures

It is important to determine the refraction index values of the glass structures to be used in the technology. The Spectroscopic Ellipsometry Technique is used to determine the optical constants of glass structures produced. The refraction index spectrum obtained as a result of measurements taken in the 400–1000 nm wavelength range for prepared glass structures is provided in Fig. 6. The addition of V_2O_5 to the base glass structure other than 1% has significantly increased the refraction index values. In addition, as the wavelength increases in these glasses, the refraction index change is noticeably different. For the 1% V_2O_5 doped silicate glass structure (S1), the values are almost the same as the base glass structure. This result supports our interpretation of the FTIR results. The non-bridging oxygen density in the structure plays a significant role in the value of the refraction index. In contributions, up to 1% to the base glass structure, the NBO in the structure is increasing and the V_2O_5 is a modification. With a 1% contribution, the V_2O_5 plays a network-building role, reducing the amount of NBO in the structure to other glasses. The refractive index and average extinction coefficient values for all glasses at 600 nm are given in Table 2.

3.4. Thermal properties

The acquisition of the DTA spectrum in the investigation of thermal properties is very useful in determining structural changes in glass compounds. The initial temperature of the first endothermic peak observed in this spectrum gives the glass transition temperature (T_g). At higher temperatures, there is a single exothermic peak attributed to the glass crystallization temperature (T_C) and then an endothermic peak (T_m) caused by the glass melting. The DTA spectrum of the S0 glass structures produced is provided in Fig. 7. In addition, the temperature of the glass transition, crystallization, and melting of all-glass structures are listed in Table 3.

The temperature glass transition is very sensitive to any changes in the number of coordination of network-forming atoms and the formation of non-bridging oxygen. When Table 3 is examined, it is seen that the glass transition temperatures vary between 596 and 607 °C. T_g values have fallen to 1% V_2O_5 contribution and have increased again in the glass with 1% V_2O_5 additives. This change indicates that non-bridging oxygens (NBOs) to the S1 glass are decreasing. This result is consistent with the results we have achieved for structural and optical properties. This creates a tighter glass structure and increases the glass transition temperature. Melting temperatures (T_m) are also reduced to 1% V_2O_5 doped glass, increasing again in S1 glass, which reinforces this result. The regular increase in crystallization temperatures (T_C) as the V_2O_5 contribution increases indicates that the V_2O_5 acts as the nucleating agent.

Another value to be obtained from the DTA spectrum is the value ($T_C - T_g$), a parameter representing the thermal stability of the glass against devitrification [34–36]. The difference between T_g and T_C provides a simple way to assess the stability of the glass and is an important parameter. Thermal stability $\Delta T = T_C\text{-}T_g$ is defined as the resistance of the glasses against devitrification during the annealing (especially close to or faintly above T_g). The wide temperature range between vitreous transition and crystallization of glasses allows preforms to be designed without the risk of causing recrystallization. Therefore, it is assumed that the glass can be properly shaped if $\Delta T > 100$ °C [37]. The thermal stability values of the glasses produced in our study were determined in the range of 315–330 °C.

4. Conclusion

Novel glasses of composition 55 SiO_2 – 25 Na_2O – 5 CaO − 10 ZnO – (5 – x) MgO: xV_2O_5 (x = 0, 0.1, 0.3, 0.5, 1) were prepared by traditional melt-quenching technique. The glasses' physical, structural, optical, and thermal properties have been examined. After some measurements and calculations, the V_2O_5/MgO substitution (with the V_2O_5 increase) in the glass structure resulted in the following results:

- The densities of the glasses have been slightly reduced and the molar volumes have increased.
- The pics in the FTIR spectrum were interpreted and the 1% V_2O_5 contribution was found to play a glass-former role in the structure.

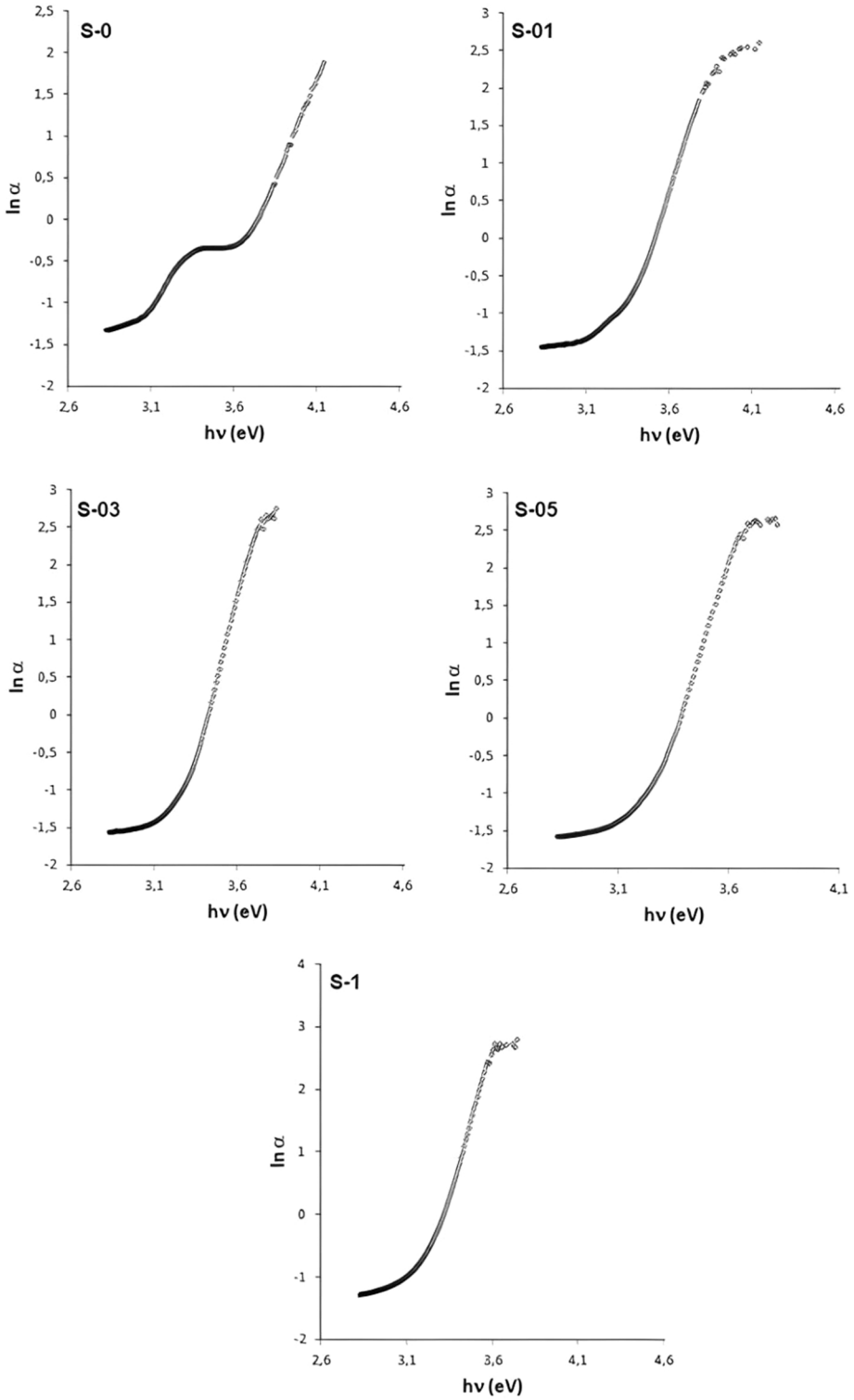


Fig. 5. ln α ~ hν graphs of the produced glasses.

– Optical transmittances in the visible region are close to 90%, and increasing the V_2O_5 contribution did not show a significant decrease in transmittance.
– When V_2O_5 is doped, it is observed that there is a significant decrease in the optical band gap (E_g) value of the glass structures up to S-1 glass. No significant change was observed in the E_g value of 1% V_2O_5 doped S-1 glass.

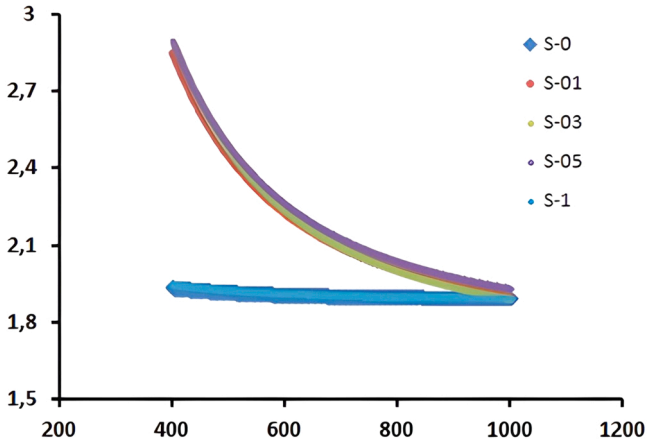


Fig. 6. Refractive index spectrum of the produced glasses.

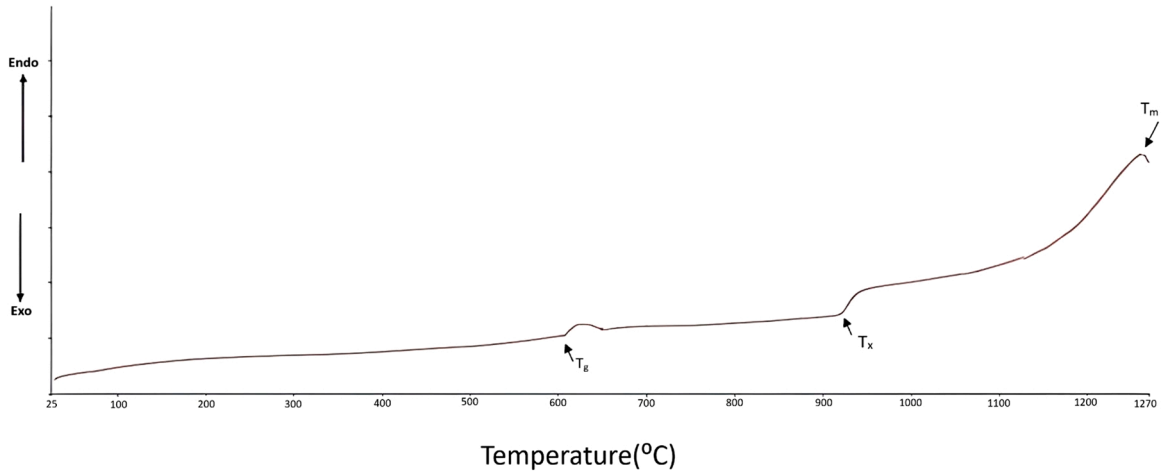


Fig. 7. DTA spectrum of the S0 glass.

Table 3
Values for glass transition temperature (T_g), crystallization temperature (T_C), melting temperature (T_m), and thermal stability (T_C-T_g) for silicate glass structures.

Sample	T_g (°C)	T_C (°C)	T_m (°C)	T_C - T_g (°C)
S-0	607	922	1263	315
S-01	602	925	1260	323
S-03	600	929	1256	329
S-05	596	934	1255	338
S-1	605	935	1261	330

- By calculating Urbach energy values, defined as the width of the localized tail levels, the structure has become smooth and stable by increasing the V_2O_5 ratio in the glass network.
- The refractive indices of the produced glasses at 600 nm vary between 1.916 and 2.264. It was concluded that the amount of NBO in the structure increased when V_2O_5 was added up to 1% to the base glass structure and that the 1% contribution of V_2O_5 also played a glass-forming role.
- Glass transition, crystallization, and melting temperatures of glasses were determined by thermal analysis. In addition, thermal stability values were also calculated. From the results obtained, again, it was observed that the 1% V_2O_5 doped glass showed different changes from the other glasses. According to the thermal stability values, the glasses we produce allow to be designed without the risk of recrystallization.

Declaration of Competing Interest

The authors declare that they have no known competing financial interests or personal relationships that could have appeared to influence the work reported in this paper.

Data Availability

Data will be made available on request.

Acknowledgments

The author is thankful to Eskisehir Osmangazi University Scientific Research Projects Commission for providing financial support under project number 202019019.

References

[1] A.D. Neamen, Semiconductor Physics And Device, McGraw-Hill, 2003.
[2] J.A. Benjamin, G.S. Moulton, Encycl. Mater.: Tech. Ceram. Glass (2021) 462–482.
[3] D.E. Flügel, Properties of zinc silicate glasses and melts, J. Mater. Sci. Eng. A (2011) 312–320.
[4] C.S. Lee, M. K, Fabrication and characterization of glass and glass-ceramic from rice husk ash as a potent material for Opto-electronic applications, J. Mater. Sci. -Mater. Electron (2017) 17611–17621.
[5] S.A.A. Wahaba, K.A. Matori, et al., Effect of ZnO on the phase transformation and optical properties of silicate glass frits using rice husk ash as a SiO2 source, J. mater. Res. Technol. (2020) 11013–11021.
[6] S. Ye, E.-H, S.-Y, Transition metal-involved photon upconversion, Adv. Sci. (2016).
[7] J. Qiu, Controlling the metastable states of glasses by external fields, Int. J. Appl. Glass Sci. 7 (3) (2016) 270–284.
[8] C. Lin, L. L, Oxyfluoride glass-ceramics for transition metal ion based photonics, J. Phys. Chem. C (2016) 4556–4563.
[9] M.A. Marzouk, S. A.-N, Glass former effects on photoluminescence and optical properties of some heavy metal oxide glasses doped with transition metal ions, J. Appl. Spectrosc. 84 (2017) 162–169.
[10] F.H. ElBatal, M. M, Gamma rays interaction with bismuth borate glasses doped by transition metal ions, J. Mater. Sci. 46 (2011) 5140–5152.
[11] E.M. Ahmed, N. E.-G, Electrical conduction and switching properties of As2O3·V2O5·FeO glasses, J. Mater. Sci. Mater. Electron. 29 (2018) 15191–15202.
[12] E.M. Ahmed, N. E.-G, Effect of Nd3+ ions on the structural, physical, and emission properties of, Ceram. Int. 46 (2020) 25089–25096.
[13] H.O. Tekin, S. A, A systematical characterization of TeO2–V2O5 glass system using, Appl. Sci. (2021) 3035.
[14] R. Balaji Rao, N. Veeraiah, Study on some physical properties of Li2O-MO-B2O3: V2O5 glasses, Phys. B Condens. Matter 348 (2004) 256–271.
[15] A. Paul, Chemistry of Glasses, Springer, Netherlands, 2012.
[16] I. Kashif, A. A.-M, Effect of Nd2O3 addition on structure and characterization of lead-bismuth borate glass, Results Phys. 4 (2014) 1–5.
[17] T. Liua, L. C, Characterization of structure and properties of MgO-Al2O3- SiO2-B2O3-Cr2O3 glass-ceramics, J. Non-Cryst. Solids (2020), 120154.
[18] L. Deng, Z. W, Crystallization behavior and structure of CaO–MgO–Al2O3–SiO2 glass-ceramics prepared from Cr-bearing slag, Mater. Chem. Phys. (2021), 124249.
[19] B. Mehdikhani, Effect of V2O5 additions on the crystallization of sodium silicate glasses, Glass Technol. Eur. J. Glass Sci. Technol. Part A (2012) 146–149.
[20] Praveen Jha. (2017). Preparation and Characterization of SiO2-CaO- MgO-K2O Glasses as Biomaterials. http://hdl.handle.net/10266/4922.
[21] S.A. Abdul Wahab, M. K, Effect of ZnO on the phase transformation and optical properties of silicate glass frits using rice husk ash as a SiO2 source, J. Mater. Res. Technol. (2020) 11013–11021.
[22] T. Annapurnaa, K. M, Polaronic conduction and dielectric relaxation dynamics in V2O5 added to lead-bismuth silicate glass system, J. Non-Cryst. Solids (2020), 119746.
[23] Q. Chen, Optical linear & nonlinearity and Faraday rotation study on V2O5 nanorod doped glass and glass-ceramic: Impact of optical basicity, J. Alloy. Compd. (2020), 155490.
[24] A.J.A. Al- Nidawi, K.A. Matori, A. Z, Effect of MnO2 doped on physical, structure, and optical properties of zinc silicate glasses from waste rice husk ash, Results Phys. (2017) 955–961.
[25] M.H. Mohd Zaid, M. K, A comprehensive study on compositional dependence of optical band gap in zinc soda-lime-silica glass system for optoelectronic applications, J. Non-Cryst. Solids (2016) 107–112.
[26] E.M.A. Khali, E. B, Infrared absorption spectra of transition metals-doped soda-lime-silica glasses, Phys. B: Condens. Matter (2010) 1294–1300.
[27] G.V. Sarrigani, Q. H, Characterization of waste material derived Willemite-based glass-ceramics doped with erbium, Adv. Mater. Sci. Eng. (2015) 1–7.
[28] I.M. Alibe, M. K, Effects of calcination holding time on properties of wide band gap Willemite semiconductor nanoparticles by the polymer thermal treatment method, Molecules 23 (*4*) (2018) 873.
[29] V.N. Sukhanov, Optical properties of porous glass modified with vanadium(V) Oxide, Russ. J. Appl. Chem. 76 (2003) 1201–1204.
[30] S. Sindhu, S. S, The role of V2O5 in the modification of structural, optical, and electrical properties of vanadium barium borate glasses, Phys. B 365 (2005) 65–75.
[31] S. Yusub, N. T, Structural investigation of vanadium ions doped Li2Osingle bondPbOsingle bondB2O3single bondP2O5 glasses by means of spectroscopic and dielectric studies, J. Mol. Struct. 1076 (2014) 136–146.
[32] A.M. Abdelghany, H. A, Impact of vanadium ions in barium borate glass, Spectrochim. Acta A 137 (2015) 39–44.
[33] F.H. Hammad, The role of V2O5 on the structural and optical properties of MgO-ZnO-CdO-P2O5 glasses and the impact of gamma irradiation, Silicon 10 (2018) 831–840.
[34] Fatma H. Margha, G. T.-B, Enhancing the electrical conductivity of vanadate glass system (Fe2O3, B2O3, V2O5) via doping with sodium or strontium cations, Ceram. Int. 45 (2019) 11838–11843.
[35] D. Uhlmann, Glass formation, J. Non-Cryst. Solids 25 (1977) 42–85.
[36] M. Saad, M. P, Glass forming ability criterion, Mater. Sci. Forum Trans. Tech. Publ. (1987) 11–18.
[37] S.F. Hanane Barebita, Structural investigation of Bi2O3-P2O5-B2O3-V2O5 quaternary glass system by Raman, FTIR, and thermal analysis, Chem. Phys. Lett. (2020), 138031.